Nanotechnology Perceptions
ISSN 1660-6795
www.nano-ntp.com

FEATURES OF SILVER THIN FILMS APPLIED ON FTO GLASS PLATE FOR DYE-SENSITIZED SOLAR CELLS USING GREEN SYNTHESIS AND CATHARANTHUS ROSEUS LEAF EXTRACT

DEEPA.G[1]Dr O.N. Balasundaram[2]

[1]Research Scholar, Department of Physics, Research & Develoment Centre
Bharathiar University Coimbatore , Tamilnadu
[2]Associate Professor
Department of Physics, PSG College of Arts and Science
(Affiliated to Bharathiar University), Coimbatore, Tamilnadu

Abstract

Silver thin films accumulated on an FTO-coated glass substrate with different molar concentrations using the spray pyrolysis process. Silver-nanostructured films are deposited using Catharanthus roseus leaf extract and silver nitrate solution. According to the study, growth and shape/size are significantly influenced by the silver thin film method's response time. Silver thin films have been studied using the UV-visible spectrophotometer, Photoluminescence [PL], Field Emission Scanning Electron Microscope (FE-SEM) with EDX, X-Ray Diffraction (XRD), and finally AFM techniques. Lastly, these films are effectively applied in dye-sensitized solar cells.

Keywords: -XRD, silver, FTO glass plate, and Catharanthus roseus.

1. INTRODUCTION

Gratzal and his generations were the ones who originally developed the Dye Sensitized Solar Cell (DSSC), a third generation photovoltaic cell, in 1991 [1, 2]. Considering its low production costs, ease of assembly, and environmental friendliness, DSSC has drawn a lot of attention. An inorganic semiconducting metal electrode, an electrode counter, an electrolyte, and a color sensitizer make up a DSSC.[3].Since the development of DSSC, numerous novel strategies have been developed to achieve high-performance DSSC with enhancements to counter electrodes, electrolytes, dyes, and photo anode semiconductor materials. The photo anode is one of them that is essential to the cell's operation [4]. The synthesis of green pathway Ag thin films is the subject of this article. Green synthesis contains effective noble metals as well as synthetic thin films [5-8].In order to provide environmentally acceptable techniques for thin film synthesis, the utilization of biological approaches has emerged as a new technique [9]. Plant-based synthesis has developed as a simple and practical substitute for physical and chemical processes. It has been established that the plant extract possesses reducing and stabilizing properties [10]. Dye Sensitized Solar Cells (DSSCs) are becoming a hot topic for research because of their affordability and ease of use. [11]. The efficiency of dye-sensitized solar cells (DSSCs) is low when compared to photovoltaic cells. Various efforts are being done to identify an efficient dye near serve via a sensitizer for photocurrent increase. A recent study using DSSC leaf dye extract reported an efficiency of photoelectric energy conversion [12].

***Catharanthusroseus*uses**

Herbal medicines containing periwinkle have been used to treat wound healing, depression of the central nervous system, and muscle soreness. His applications range from treating stomach-aches to preventing

diabetes. The non-toxicity technique is the green synthesis option, which is why I chose this topic for the current study. Silver films at different concentrations build up in FTO glass plates. It looks into the morphological characteristics, optical qualities, and arrangement of impact film concentrations, among other things. Finally, his dye made the energy transfer to the solar cell more sensitive.

2. Experimental Details

2.1. Materials

All regents were of analytical grade with 99% purity. Silver nitrate [$AgNO_3$] was boughtfrom Subra scientific company, Pondicherry, India. All chemicals and reagents were used as acquired without in addition purification. Deionized water was used inallexperimental work.

2.2. Collections of leaf

Every regent was 99% pure and of analytical quality. The supplier of AgNO3 (silver nitrate) was Subra Scientific Company in Pondicherry, India. Without further purification, all chemicals and reagents were utilized just as they were purchased. Every experiment that was conducted used deionized water.

2.3. Preparation of leaf Extract

After gathering the fresh Catharanthus roseus leaves, they were properly washed in both tap and distilled water to get rid of any dust and undesirable visible particles. The leaves were finely minced after they had dried fully. For an hour, each 10g of chopped Catharanthus roseus leaves were continuously stirred while boiling in 50 ml of distilled water at 60°C. At this point, the watery portion becomes a light green or pale yellow tint. The extract was allowed to cool before being filtered using what man no. 1 filter paper and kept for later use at 4°C. It served as a stabilizing and reducing agent.

2.4. Preparation of the substrate and material

Glass measuring 50x50x2.2 mm served as the FTO substrates. To identify the pyrolysis region that was sprayed, one of the controls was clipped. They were first cleaned with soap to get rid of the clay and then left in a beaker with nitric acid for half an hour. The cleaned substrates were then dried in the oven for a whole night before being used for thin film.

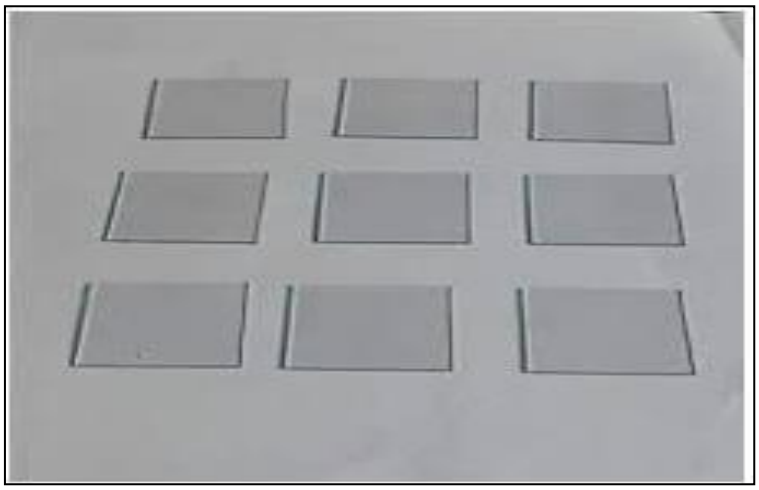

Fig:1.Fluorinedopedtin oxidecoatedglassslides50x50x2.2mm

2.5. Preparation of silver thin films

Various quantities of silver (AgNO3) at 0.025, 0.05, 0.075, and 0.1 M were utilized as a precursor solution. It is used with 50 milliliters of deionized water that has been pelletized and rotated for ten minutes. It is then placed in a beaker and individually administered at room temperature with five milliliters of Catharanthus roseus leaf extract. After 15 minutes, the solution changed from reddish brown to yellow, indicating the creation of silver.Experimental configuration for the deposition of thin silver films onto the FTO glass substrate. The substrates were heated for a predetermined amount of time before the synthetic solvent was sprayed on them, in preparation for the deposition. Measurement of the conductive content of FTO glass plates using a digital multimeter. The glass substrate was properly adhered to, and the silver films obtained with the aforementioned concentration were standardized. The spray coating conditions were maintained consistent throughout the whole silver thin film deposition process. Samples were taken and

annealed for two hours at 300 °C in the muffle furnace after cooling. Finally, a description of the deposited thin films is given.

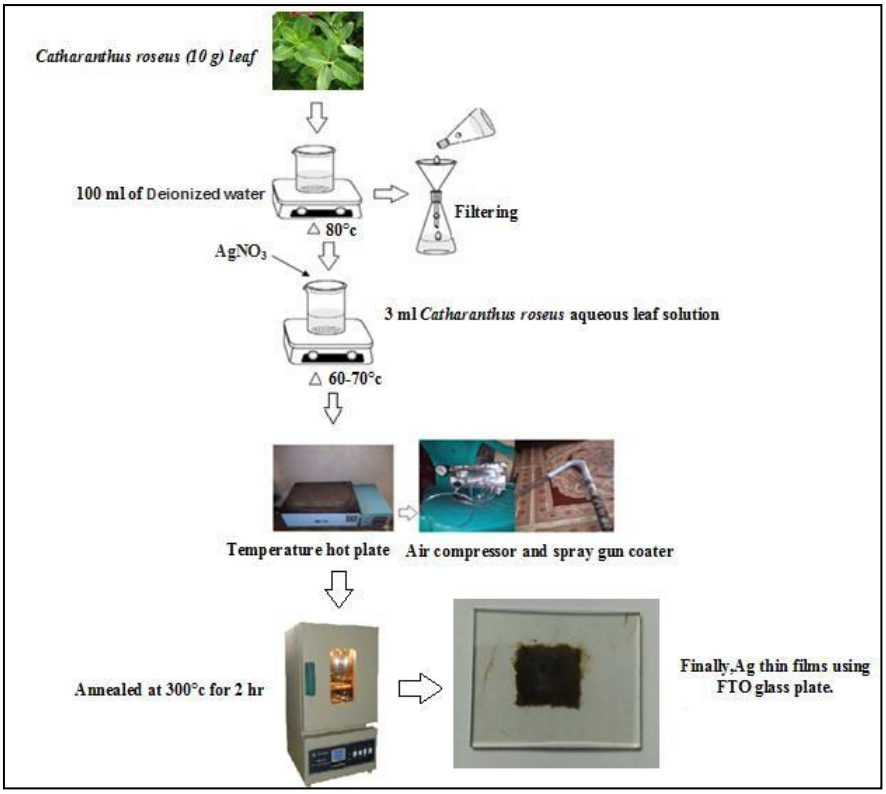

Flowchart for the preparations of FTO glass platesilver thin film

Characterization technique used

The green generated thin films were examined using a variety of microscope and spectroscopic instruments. The X-Ray Diffraction (XRD) approach was utilized to confirm the thin films initially. It involved fitting a monochromatic Cu-KAl radiation (λ = 1.5406 A°) with a SHIMADZU-6000 for structural categorization of the deposited films. The JEOL 6300 field emission scanning electron microscope (FESEM) was used to study the surface morphology. Using an AGILENT-N9410A-5500 (Nano Surf Simple Scan 2), topological analysis Atomic Force Microscopy (AFM) was performed in the 300–1200 nm range with a JASCO V-670 spectrometer. Solar energy was used to record optical absorption spectra (UV-Vis) under illumination conditions. The DSSC's current density-voltage (J-V) characteristics were measured under AM 1.5G and 100 mW cm-2 using the Keithley 2450 Source Meter and the SS50AAA (Photo Emission Tech) solar simulator.

Fig:2.Photographical image of J-Vanalyzer (Keithley2450)

3. Results and Discussion

3.1. Structural study

X-ray diffraction was used to characterize the thin films' crystalline structure and phase identification. The silver thin films that were biosynthesized using leaf extract from Catharanthus roseus were validated by the distinctive peaks seen in the XRD patterns, as displayed in Figure 3.Four distinct molar concentrations of silver thin sheets (0.025, 0.05, 0.075, and 0.1 M).Silver is totally soluble because the other peaks, such the silver FTO peaks, are suppressed. Within the examined composition spectrum [13].Ag enhances the (101) plane's intensity, which is higher than the pure silver thin film's intensity. The reason for this is that it indicates that the One hundred and one silver thin-film planes placed on FTO is higher on coated glass than it is on pure Ag film put on the film, indicating improved crystallinity. Thus, the concentration for film is indicated by the emergence of the Ag peak.

A decrease in amorphous concentrations is trended by the XRD. When compared to the JCPDS data card [04-0783], the limit is indicated as Face Centered Cubic (FCC) Silver (111). The Scherer relationship is utilized to ascertain the crystallite concentration of 0.1 M:

TheusingScherer'sformula,crystallitesizeDisdetermined.

$$D = \frac{k\lambda}{\beta\cos\theta} \quad \text{.. . . . . (1)}$$

The wavelength employed is k (1.5405 A °), the full half-limit width (FWHM) is expressed in radians B, and the angle of Braggs is expressed in radians h, where the form factor is k = 0.9.At 0.1 M concentration, the size of the crystallites for the (111) plane was determined to be 19 nm. Consequently, the green synthetic thin silver films, whether nanocrystalline or amorphous, are clearly visible in the XRD patterns [14].

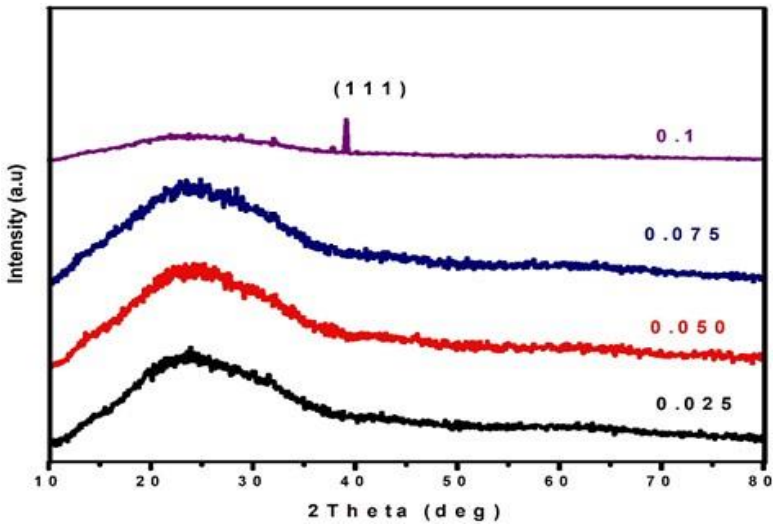

Fig:3.XRDpatterns of thesprayedsilverthinfilmsatdifferent molarconcentrationsof *Catharanthusroseus* leafextract.

3.2. Opticalstudies

Absorption spectra of four distinct leaf extract concentrations on silver thin films. Figure 4 displays optical absorption spectrum thin sheets in silver covering the 200–800 nm spectral range.Up to 413 nm, the film spectrum is observed. This implies a strong reliance on visible range silver concentrations. This is because of well-crystallization in the case of silver thin films, when the concentration rises [15]. absorption in pure film as a result of both the messenger's photon absorption and the increase in crystal defects of the scattered photon. Therefore, 0.1M silver thin film is optimal for use [16].Equation (2) was utilized to determine the energy band gap of silver thin films.

$$\textbf{Band gap energy} = \frac{hc}{\lambda} \qquad \text{----------(2)}$$

Where, h is the planks constant, c is the rate of mild and λ is the wavelength fromthis, it's farshowedthatas awarenesswillincreaseparticlesizedecreaseswhichmaybeduetoblueshiftinabsorbancepeaks.

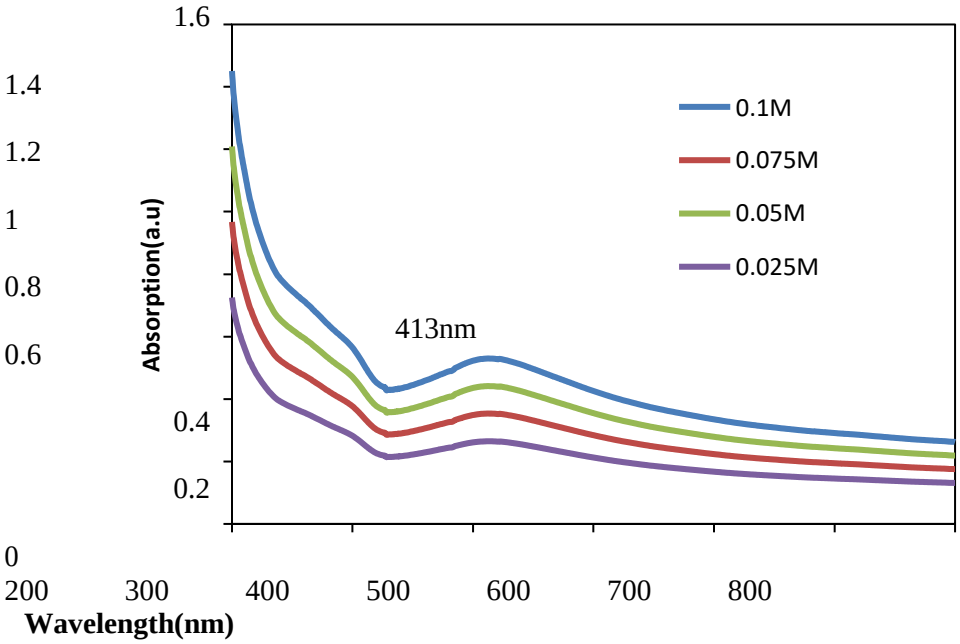

Fig:4.Opticalabsorptionofvarious thin silverfilm concentrationsof *Catharanthusroseus* leafextract.

3.3. Opticalbandgap

To measuregraph $(\alpha h\square)^{1/2}$ Vs photon energy (h□) shown in Fig: 5.Indicates the energyband difference from absorption spectra. Silver has an absorption coefficientα obeying thefollowingrelation, as adirect band gap.

Theopticalbanggap energywasdeterminedusingTaucmode

$l(\alpha h\square)=A\ (h\square-Eg)^{½}$ ---------- (3)

WhereCisconstant,theenergyofthebandgapisEg,andthefrequencyofthephoton is□.

The results also indicate that when silver thin films have higher bandgap energies of 2.8, 3.0, 3.6, and 3.8 eV, the absorption band edge shifts towards the visible area. These findings imply that silver might be integrated into the electrical characteristics of the crystalline silver band structure [17]. The optical results suggest that silver could boost the silver DSSC and enhance visible light absorption.

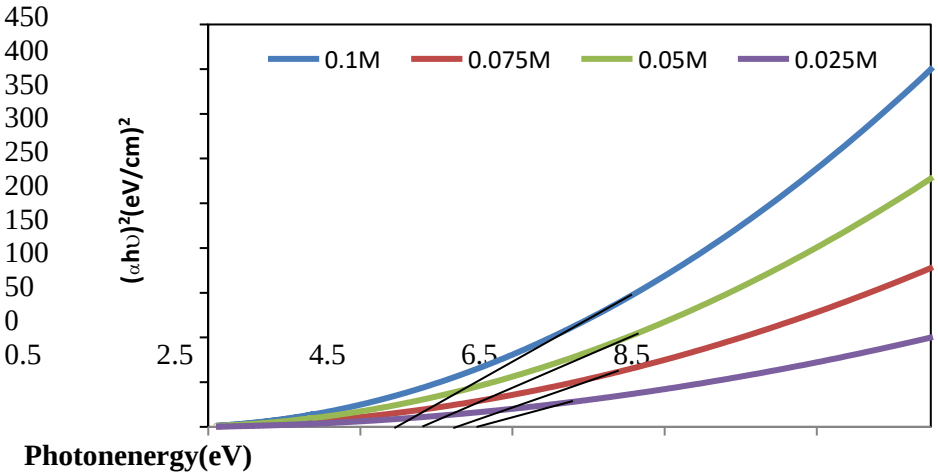

Fig:5.(αhν) Vshν plotof thesilverthinfilmsof*Catharanthusroseus* leafextract.

3.4. Photoluminescence(PL)spectrumstudy

The photoluminescence (PL) technique is appropriate for evaluating the crystalline content and contaminants in the products. It has been discovered that the produced colloidal silver thin sheets exhibit photoluminescence [18].PL spectra on the glass layer for the silver thin films. It is proven that the PL peak occurs at 490 nm for all silver thin film concentrations. It was previously shown that the visible silver thin film luminescence was caused by stimulation. Figure 6 shows that for A shift in the location of (max=490 nm) is observed at varied concentrations of silver films, indicating steady and reliable deposition of silver thin films.

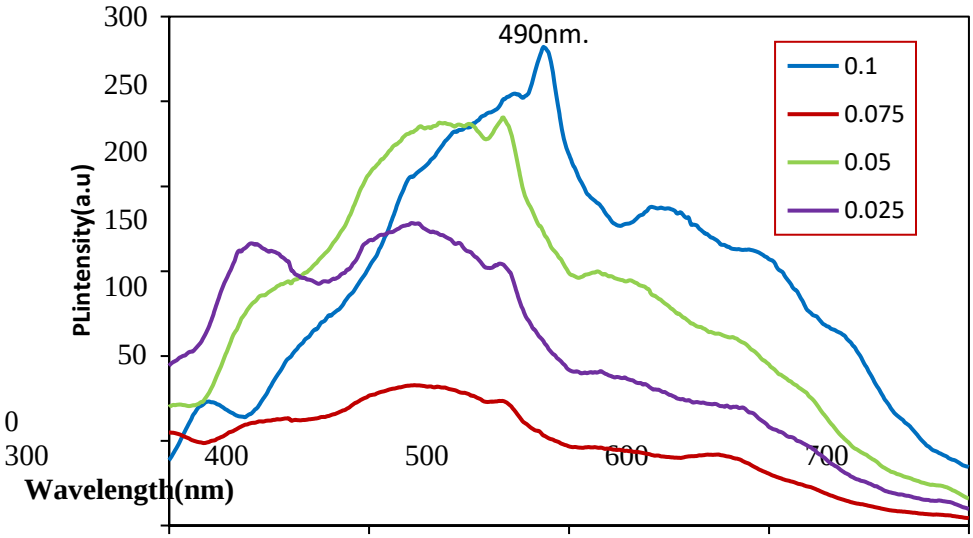

Fig: 6.Silver thin films photoluminescence emission spectrum of *Catharanthus roseus* leafextract.

3.5. Morphologicalstudies

Using FE-SEM micrographs, the surface morphology of the artificially produced silver thin films was investigated.The surface evolution of the FTO glass plate silver deposition of thin layers was described by FE-SEM studies, as Fig. 7 illustrates.The microstructure of the film is a broad spherical with a non-uniform distribution [19].The films with uniform distribution at 0.1 M of Ag have a small-sized surface with no voids or cracks that makes it appropriate for DSSC. The surface is covered with thin silver films, and the dye-sensitized solar cells in the dye will powerfully sensitize and absorb more dye molecules from these spherically shaped films.

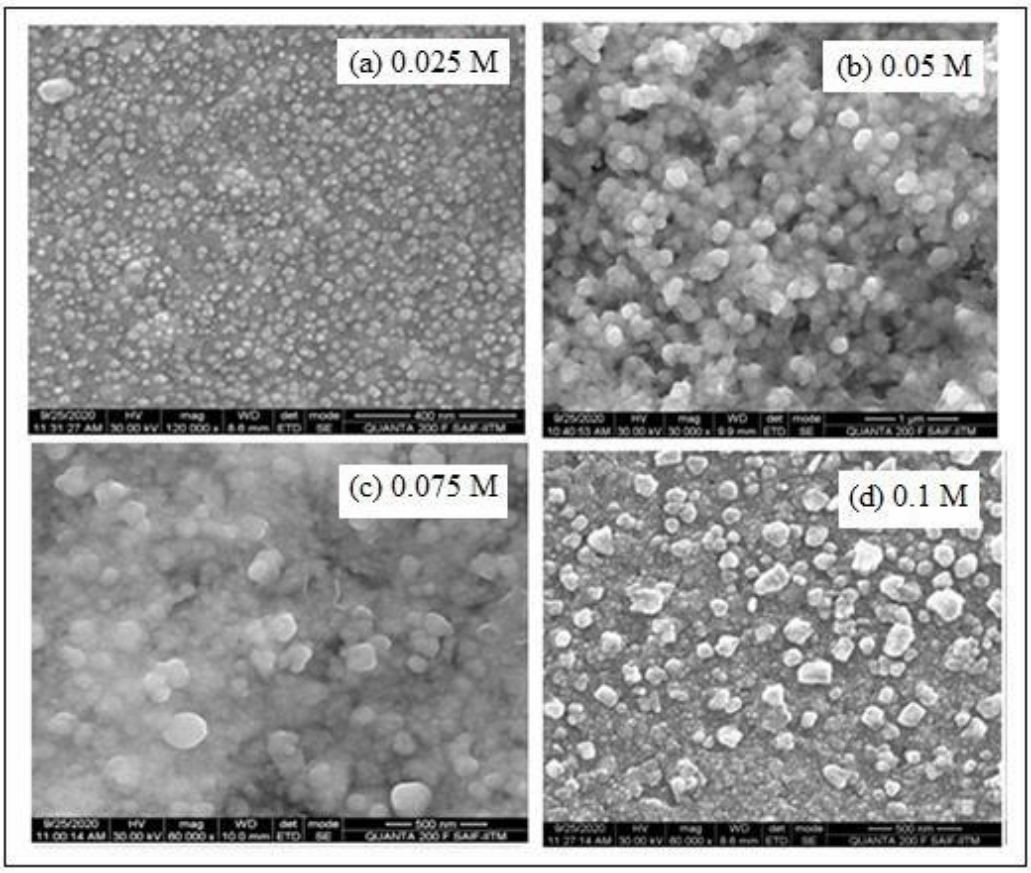

Fig: 7.FE-SEM images of silver thin films of varying molar concentrations of *Catharanthusroseus*leafextract.

3.6. Compositionalanalysis

Both the qualitative and quantitative status of the elements that might be involved in the creation of thin films is provided by EDX analysis. Table 1 displays the proportion and weight of the constituents in the suspension.Figure 8 illustrates how the Energy Dispersive X-Ray examination verifies the presence of C, N, O, Ca, Mg, Si, P, O, and Ag.Ag is seen in the EDX spectrum because to the FTO coating on the glass plates.EDX was used to assess a study of cleansilver thin films at a concentration of 0.1 M (a representative sample). [20].On the surface of the thin films, the profile of the distinctive silver peaks is emphasized. recommending the effective use of plant leaf extract in the fabrication of silver thin films.

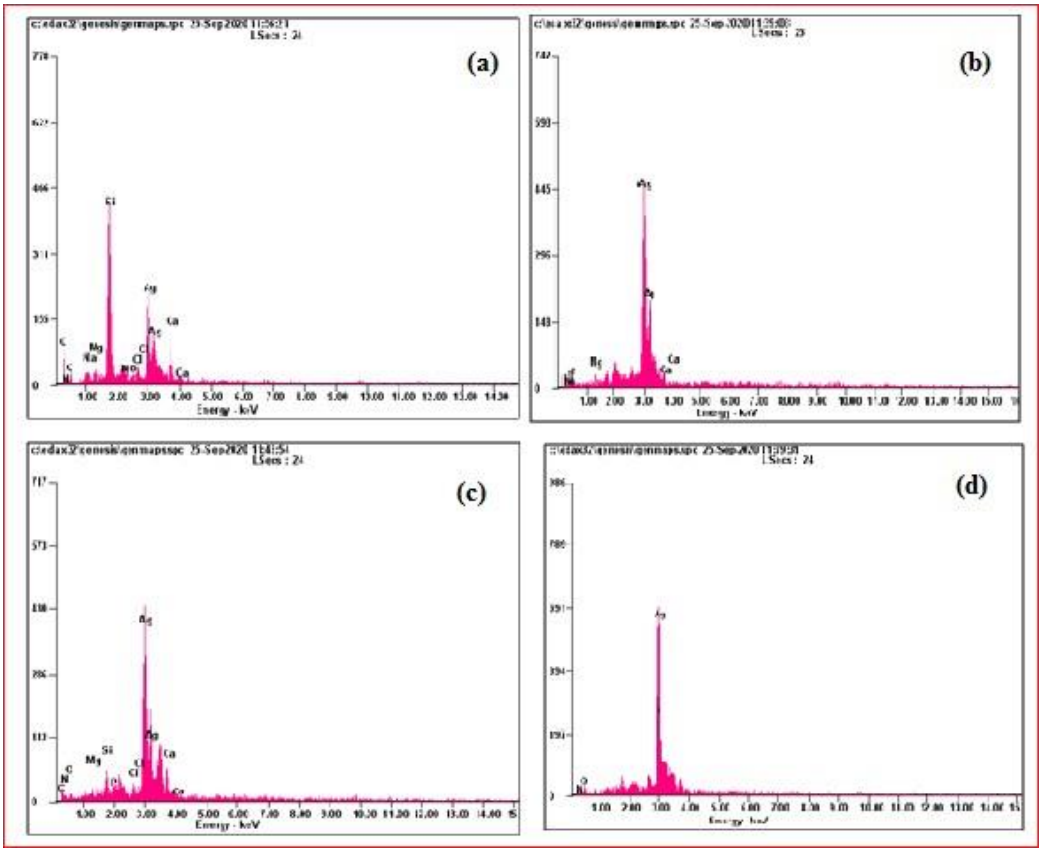

Fig:8.EDXspectrumat variousmolarconcentrationsofthesilverthinfilmsdepositedontheFTO glass plateof Catharanthus*roseus* leafextract.

Table:1. EDXcurvewith ninedominant peaksforC,N, O,Mg, Si, P, Cu, Ca andAgrespectively.

Elements	**Weight %**	**Atomic%**
CK	09.07	31.23
NK	02.75	08.12
OK	07.72	19.95
MgK	02.33	03.96
SiK	02.54	03.73
PK	01.55	02.07
CUK	01.24	01.45
CaK	02.44	02.51
AgL	70.37	26.98
Total	100.00	100.00

3.7. AFM

Silver film pictures were created using Atomic Force Microscope (AFM) (2D) examinations at concentrations of 0.025, 0.05, 0.075, and 0.1M accumulated on the FTO glass substrate depicted in fig. 9(a) [21]. With a surface roughness value of 146 nm, a topographic AFM image shows continuous growth of silver thin films on the glass surface via different irregularly spaced 100 nm silver sizes with heights of 70, 130, 160, and 225. The mushroom-like development can be seen in the 3D image of fig. 9(b) in the movie [22]. However, the three-dimensional picture at greater molar concentrations shows a randomly distributed particle size. It is evident from the morphological and topographical investigations that the film is appropriate for use in solar cell and DSSC applications.

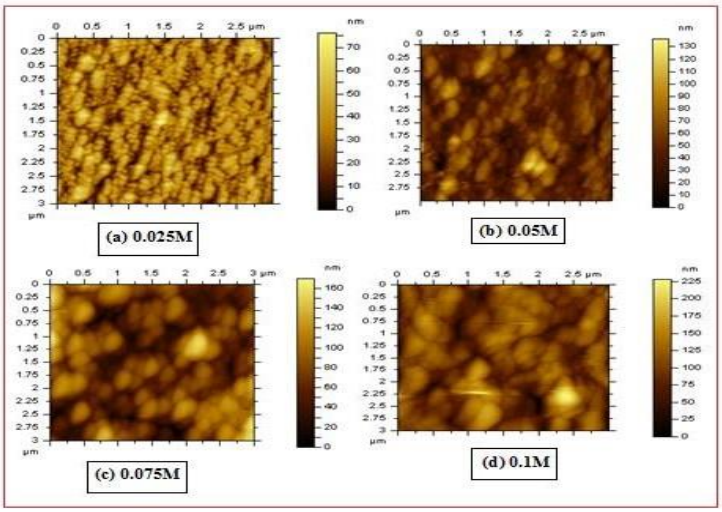

Fig:9.(a)AFM(2D)imagesofAg filmsatdifferentconcentrations of*Catharanthusroseus*leafextract.

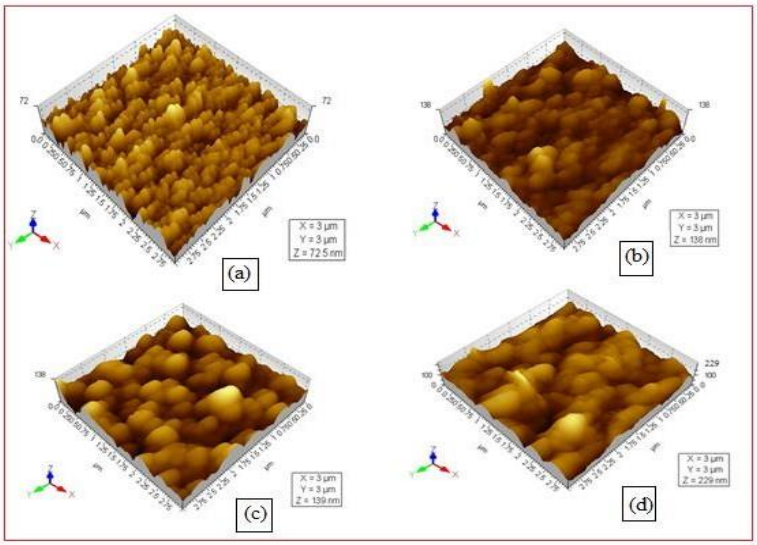

Fig:9(b)AFM(3D)imagesof Agfilmsat differentconcentrationsof*Catharanthus roseus*leafextract.

4. Application

4.1. DyeSensitizedSolarCell(DSSC)

Figure 10 illustrates the working theory of the DSSC.wherein the Ag and the dye molecules create their inorganic-organic contacts. The conductive glass absorbs solar light, and the dye (photosensitizer) that is sensitive to solar (visible) light absorbs the photon. Via the external wire, the dye electron is moved into Ag's conduction band and enters the load (e.g. lamp).The redox iodide (I-) oxidized (I3-) reaction and the electron release from the electrolyte will substitute for the dye electron loss. The electron from the load is recycled back into the DSSC during the process of converting light into electrical energy by passing through the counter (Ag coated FTO), which catalyzes the reduction reaction of the electrolyte tri-iodide (I3-) to iodide (I-). [23].

In this work, the DSSC's electrical efficiency was improved by its large active surface area. when was already mentioned, the DSSC's efficiency grew when the dye and electrolyte levels rose in tandem with an increase in Ag's active surface area, content, and light penetration.

In general, the power density has declined over time along with the voltage and current densities. Power densities peaked on days three and six because voltages often peaked on day two, while current densities peaked on days three and six. To lessen power drops, the finest DSSC sample was wrapped around plastic packaging.A comparison and plot of the power density performances are shown in fig. 11. While there was only a slight reduction in power density, the power density output could not be significantly stabilized, the plastic rapping did help. The power density dropped as a result of the vaporizations of our original idea, which involved a dye and electrolyte solution. Still, it appeared to be the cause of the decline rather than merely solution vaporizations. Power generation may also have been impacted by dye and electrolyte solution instability, such as dye degradation and irreversible electrolyte redox reaction [24].

Using photocurrent density-voltage (J-V) plots as prepared photo anodes of Ag thin films by 0.025, 0.05, 0.075, and 0.1 M concentration values of DSSC, the photovoltaic output was investigated. The Ag is used in the manufacturing of solar cell performance characteristics, which are derived from the dye produced from Catharanthus roseus [25]. The data indicates that the base cell produces the greatest results when dye is applied as a sensitizer to Catharanthus roseus with Ag. The information clearly shows that Catharanthus roseuswith silver.

In terms of voltage open-circuit (Voc), fill factor (FF), current density short-circuit (Jsc), and fill factor (FF) performance, dye attains the highest value as a sensitizer. It is observed that because dye molecules have a lot larger volume than silver thin film, cell efficiency based on photo electrodes is significantly better than cell efficiency based on pure photo electrodes. [26].

$$\square\square = \frac{J_{SC} V_{OC} FF}{P_{in}} \qquad \text{…..(4)}$$

Pintheenergyofthephotonincidentdenotes

$$FF = \frac{J_{max} \square V_{max}}{J_{SC} \square V_{OC}} \qquad \text{…..(5)}$$

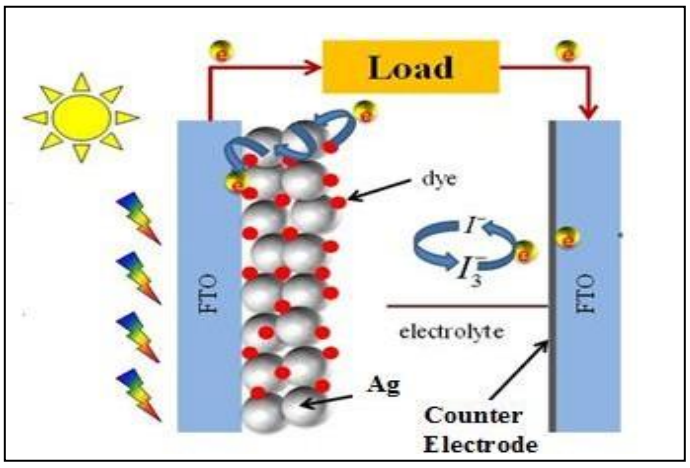

Fig:10.Schematicdiagramofthedyesensitizedsolarcellworkingtheory.

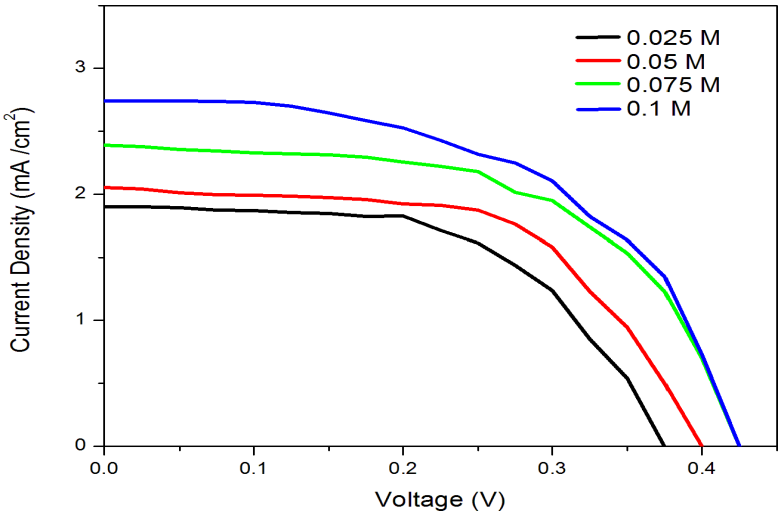

Fig:11.J-V characteristics of dye sensitized silver thin film of *cathranthus rosues* leafextract.

Table.2DSSCwithelectrodeofAgthin Filmsderivedfrom thedyeextractedfrom

Catharanthusroseus

Molarconcentration(M)AgthinfilmofCatharanthusroseus	**Jsc(mA/cm^2)** **Shortcircuitcurrent**	**Voc(mV)** **Opencircuitvoltage**	**FF** **FillFactor**	**%** **Efficiency**
0.025	1.8	0.38	0.55	1.5

0.05	2.1	0.4	0.59	1.9
0.075	2.4	0.42	0.60	2.4
0.1	2.55	0.43	0.73	3.1

Conclusion

Spray pyrolysis techniques were used to carry out the green synthesis of silver thin films and deposit FTO conductive glass substrates. The Face Centered Cubic (FCC) was found to be strongly produced in the films deposited with silver thin film, according to XRD tests. At The movie was on the (111) plane during this focus. When silver was added, the surface morphology of the film improved. The surface roughness of the film was analyzed for silver using the AFM study.UV-visible absorption range spectrum. With increasing concentration, the optical band gap variance was caused by the different silver basis concentrations. From 2.8, 3.0, 3.6, and 3.8 eV, the band gap grew as the concentration of silver rose. Additional PL investigation confirmed the optical observation by showing a minor red alteration in the emission peaks. Using Catharanthus roseus extract's silver nanomaterial as a dye, DSSC was successfully created. It has been noted to increase fill factor and conversion efficiency. The DSSC has an efficiency of 3.1%.

References

1) O'Regan and Gratzel.M, **(1991)** .A low-cost, high efficiency solar cell based on dyeSensitizedcolloidal TiO2 films,*Nature* 353, 737–740.
2) Jinchu.I, Sreekala.C and Sreelatha K.S**(2014).**Dye sensitized solar cell using naturalDyesas chromophores,*material scienceforum*77, 39–51.
3) Chang.S and Chen.T E **(2012**).Enhancement of low energy sunlight harvesting in dyesensitized solar cells using plasmonic gold Nano rods, *Energy Environmental Science*, 5,9444–9448.
4) S.P. Lim S.P, Pandikumar .A and Lim H.N **(2014)**.Enhanced photovoltaic performance ofsilver@titania plasmonic photoanode indye sensitizedsolar cells,*RoyalSociety ofChemistryAdvances*, 4, 38111–38118.
5) SancunHao,JihuaiWu,YunfangHuang,JianmingLin**(2006).**Naturaldyesasphotosensitizersfor dye-sensitized solar cell, *Solar Energy*80,209–214
6) Khwanchit, Wongcharee, Vissanu Meeyooa, Sumaeth Chavadej **(2007)**.Dye-sensitizedsolar cell using natural dyes extracted from rosella and blue pea flowers, Solar *EnergyMaterials& Solar Cells*,91,566–571.
7) MichaelGratzal**(2003)**.Review Dye-sensitizedsolar cells,*JournalofPhotochemistryandPhotobiology C: PhotochemistryReviews*, 4, 145–153.
8) Kiruba Daniel S.G and Muthusamy and Shivakumar.P **(2013)** .Rapid synthesis of Agnanoparticles using Henna extract for the fabrication of Photo absorption Enhanced DyeSensitizedSolarCell, Advanced*MaterialsResearch,*78, 349-360.
9) Sone B.T, Manikandan .E, Maaza .M, **(2015)**.Sm2O3 nanoparticles green synthesis viaCallistemonviminalisextract,*Journal of Alloysand Compounds*, 650,357–362.
10) Thovhogi.N,Parke,andGurib-Fakim.M,**(2016)**.PhysicalpropertiesofCdOnanoparticles synthesized by green chemistry via Hibiscus Sabdariffa flower extract,*Journalof Alloys and Compounds*,655, 314–320.
11) Diallo. A, Mothudi B.M **(2016).**Luminescent Eu2O3 Nano crystals by Aspalathus linearis'extract:structuralandopticalproperties,*JournalofNanophotonics* 10, 26010–26012.
12) Solaiyammal .T, Murugakoothan .P **(2019)** .Green synthesis of Au and the impact of Auon the efficiency of TiO2 based dye sensitized solar cell, *Materials Science for EnergyTechnologies*2 , 171–180.
13) Nakaruk.AandSorrell.C**(2010)**.Conceptualmodelforspraypyrolysismechanism:fabrication and annealing of titanium thin films, *Journal of Coatings Technology andResearch*,7,665–676.
14) Shiv Shankar.S, Akhilesh Rai, Absar Ahmad andMurali Sastry**(2004)**. Rapid synthesisof Au, Ag,

and bimetallic Au core–Ag shell nanoparticles using Neem (Azadirachtaindica)leaf broth,*Journal ofColloid and InterfaceScience*,275, 496–502.

15) Dhamodharan.P, Manoharan.C, Dhanapandian.S, Bououdina.M & Ramalingam.S**(2015)**.PreparationandcharacterizationofspraydepositedSn-dopedZnOthinfilmsontoITOsubtractsasphotoanodeindyesensitizedsolarcell,*JournalofMaterialsScience:Materialsin Electronics*,26, 4830–4839.
16) Durr.M,Yasuda.AandNelles.G**(2006)**.Band-GapEngineeringofMetalOxidesforDye-SensitizedSolar Cells,*TheJournal of Physical.Chemistry. B*, 43, 21899–21902.
17) N.M. Shinde N.M and Lokhande C.D **(2014)**.A green synthesis method for large areasilver thin film containing nanoparticles, *Journal of Photochemistry and Photobiology B:Biology*,14, 1011-1344.
18) Manurunga .P, Putria.Y and Simanjuntakb.W **(2013)**. Synthesis and characterization ofchemicalbath deposited TiO2 thin-films, *Ceramics*,39, 255-259.
19) AmsterReginLawrence.R,LeonStephanRaj.T,andAntonySelvi.A**(2017)**.GreenSynthesis and Characterization of Silver Nanoparticles of Leaf Extracts of *Priva cordfolia*(L. F.)Druce, *InternationalJournal ofEcotoxicology andEco biology*,2, 52-55.
20) Jbeli.R, Boukhachem.A,Saadallah.F,and HEzzaouia**(2019**).Synthesisandphysicalproperties of Fe dopedLa2O3 thin films grown by spray pyrolysis for photocatalyticapplications,*MaterialsResearch Express,* 6, 66414-66415.
21) Fotsa Ngaffo.F, Caricato.A.P, Fernandez.M, and, Romano.F **(2007)**.Structural propertiesof single and multilayer ITO and TiO2 films deposited by reactive pulsed laser ablationdepositiontechnique,Applied,253, 6508–6511 .
22) Kokate S K, Jag taps CV, Navistar PK, Jadkar S R, PathanHMand MohiteKC**(2018).**CdS sensitized cadmium doped ZnO solar cell: fabrication and characterizations, *Optics*157, 628–634.
23) NunesVF, Santos Souzab A P, Lima F, Oliveira G, Freire FN and Almeida AF **(2018)**.EffectsofpotentialdepositionontheparametersofZnOdye-sensitizedsolarcells,*JournalMaterial Research*, 21, 53-73.
24) YaoCZ,WeiBH,MengLX,LiH,GongQJ,SunH,MaHXandHuXH**(2012)**.Controllable electrochemical synthesis and photovoltaic performance of ZnO/CdS core–shellNanorod arraysonfluorine-doped tinoxide,*JournalPowerSources*207, 222–228.
25) Kamble A et al **(2015)** .Boosting the performance of ZnO/CdS core–shell nanorod array-based solar cells by ZnS, *Advanced Materials: Israel Journal of Chemistry,* 55, 1011–1016.